

This discussion paper is/has been under review for the journal *Climate of the Past* (CP).  
Please refer to the corresponding final paper in CP if available.

# Ranges of moisture-source temperatures estimated from Antarctic ice core stable isotope records over the glacial-interglacial cycles

R. Uemura<sup>1,\*</sup>, V. Masson-Delmotte<sup>1</sup>, J. Jouzel<sup>1</sup>, A. Landais<sup>1</sup>, H. Motoyama<sup>2</sup>, and B. Stenni<sup>3</sup>

<sup>1</sup>IPSL-Laboratoire des Sciences du Climat et l'Environnement (LSCE/IPSL), UMR8212, CEA-CNRS-UVSQ, 91191, France

<sup>2</sup>National Institute of Polar Research, Research Organization of Information and Systems, Tachikawa, Tokyo 190-8518, Japan

<sup>3</sup>Department of Mathematics and Geosciences, University of Trieste, via E. Weiss 2, 34128, Trieste, Italy

\*now at: Department Chemistry, Biology and Marine Science, Faculty of Science, University of the Ryukyus, 1 Senbaru, Nishihara, Okinawa, 903-0213, Japan

Received: 27 December 2011 – Accepted: 17 January 2012 – Published: 30 January 2012

Correspondence to: R. Uemura (ruemura@sci.u-ryukyu.ac.jp)

Published by Copernicus Publications on behalf of the European Geosciences Union.

391

## Abstract

A single isotope ratio ( $\delta D$  or  $\delta^{18}O$ ) of water is widely used as an air-temperature proxy in Antarctic ice cores. These isotope ratios, however, do not solely depend on air-temperature but also on the extent of distillation of heavy isotopes out of atmospheric water vapor from an oceanic moisture source to a precipitation site. The temperature changes at the oceanic moisture source ( $\Delta T_{\text{source}}$ ) and at the precipitation site ( $\Delta T_{\text{site}}$ ) can be retrieved by using deuterium-excess ( $d$ ) data. A new  $d$  record from Dome Fuji, Antarctica is produced spanning the past 360 000 yr and compared with records from Vostok and EPICA Dome C ice cores. To retrieve  $\Delta T_{\text{source}}$  and  $\Delta T_{\text{site}}$  information, different linear regression equations have been proposed using theoretical isotope distillation models. A major source of uncertainty lies in the coefficient of regression,  $\beta_{\text{site}}$  which is related to the sensitivity of  $d$  to  $\Delta T_{\text{site}}$ . We show that different ranges of temperature and selections of isotopic model outputs may increase the value of  $\beta_{\text{site}}$  by a factor of two. To explore the impacts of this coefficient on the reconstructed temperatures, we apply for the first time the exact same methodology to the isotope records from the three Antarctica ice cores. We show that uncertainties in the  $\beta_{\text{site}}$  coefficient strongly affect (i) the glacial-interglacial magnitude of  $\Delta T_{\text{source}}$ ; (ii) the imprint of obliquity in  $\Delta T_{\text{source}}$  and in the site-source temperature gradient. By contrast, we highlight the robustness of  $\Delta T_{\text{site}}$  reconstruction using water isotopes records.

## 1 Introduction

Climate records preserved in Antarctic ice cores provide an important clue for the climate history over the several hundred thousand years. Among many deep ice cores from Antarctica, Vostok (Petit et al., 1999), EPICA Dome C (hereafter EDC) (EPICA-CommunityMembers, 2004; Jouzel et al., 2007) and Dome Fuji cores (hereafter DF) (Watanabe et al., 2003) have provided climate and environmental information covering multiple glacial-interglacial cycles.  $\delta D$  and  $\delta^{18}O$  of water have been widely used

392

as proxies for air-temperature, albeit with uncertainties in temperature reconstructions arising from possible changes in precipitation intermittency (Steig et al., 1994; Sime et al., 2009; Laepple et al., 2011), ice sheet elevation (Masson-Delmotte et al., 2011), or evaporation conditions (Boyle, 1997).

5 The latter source of uncertainty can be explored using a second-order isotopic information available through deuterium-excess ( $d = \delta D - 8 \times \delta^{18}O$ ) (Dansgaard, 1964). The  $d$  parameter gives mainly access to processes affected by kinetic fractionation and has been used as a tracer of evaporation conditions such as ocean surface temperature and relative humidity in moisture source ocean (Merlivat and Jouzel, 1979).  
10 The  $d$  value of modern atmospheric vapor above the Southern Ocean shows a clear dependency on sea surface temperature and relative humidity at the moisture source (Uemura et al., 2008). The initial information is then modified by subsequent meteorological processes (e.g. precipitation, snow formation, and cloud microphysics). The Antarctic precipitation  $d$  value is therefore also affected by kinetic fractionation during the snow formation, whose importance is expressed by a supersaturation function (Jouzel and Merlivat, 1984; Risi et al., 2010; Winkler et al., 2012), and by equilibrium distillation at very cold temperatures.

At first order, past variations of  $\delta D$  and  $d$  in ice cores can be assumed to mostly depend on polar temperature ( $\Delta T_{\text{site}}$ ), moisture source temperature ( $\Delta T_{\text{source}}$ ), and ocean isotopic composition ( $\delta^{18}O_{\text{sw}}$ ). Source and site climatic information can therefore be extracted from ice core  $\delta D$  and  $d$  records, using a linear regression model based on Rayleigh distillation isotopic model and/or more sophisticated models (Vimeux et al., 2001; Cuffey and Vimeux, 2001; Stenni et al., 2001, 2010). This dual isotope approach allows us to correct site temperature estimate for moisture source effects. Such site and source temperature inversions have been conducted with different methodologies (different adjustments of the linear regression coefficients) for Vostok (Cuffey and Vimeux, 2001; Vimeux et al., 2002), EDC (Stenni et al., 2001, 2003, 2010), and EPICA Dronning Maud Land (EDML) (Stenni et al., 2010) ice cores. These studies have revealed the importance of obliquity in modulating Vostok source temperature

393

(Vimeux et al., 2002). It has also been shown that source correction enhances the correlation between Vostok  $\Delta T_{\text{site}}$  and atmospheric  $\text{CO}_2$  during glacial inception (Cuffey and Vimeux, 2001), and that glacial millennial Antarctic Isotopic Maxima largely reflect changes in site temperature (Stenni et al., 2003). However, there is no well established methodology to reconstruct site and source temperatures.

5 Indeed, it is not possible to assess the full range of unknown source parameters (source temperature, relative humidity, wind speed) with only two isotope measurements ( $\delta D$  and  $\delta^{18}O$ ) (Stenni et al., 2010). To overcome this problem, different approaches have been deployed to account for the ocean isotope changes and relative humidity effect (Vimeux et al., 2001; Cuffey and Vimeux, 2001; Stenni et al., 2001, 2003). The largest difference between these studies lies in the coefficient describing the sensitivity of  $d$  to  $\Delta T_{\text{site}}$ , hereafter  $\beta_{\text{site}} (= -\partial d / \partial T_{\text{site}})$ , for which different studies have used values ranging from  $\sim 0.5$  (Cuffey and Vimeux, 2001; Stenni et al., 2001) to 1.2 (Salamatin et al., 2004). In this manuscript, we will review the causes for these differences and their impacts on  $\Delta T_{\text{source}}$  and  $\Delta T_{\text{site}}$  reconstructions for the three central East Antarctic ice cores using published isotope profiles from Vostok and EDC, and a new deuterium excess record from DF.

This manuscript is organized as follows: ice-core data and isotope modeling are described in Sect. 2 while causes for the  $\beta_{\text{site}}$  differences and their impacts on  $\Delta T_{\text{source}}$  and  $\Delta T_{\text{site}}$  are discussed in Sect. 3 and site and source reconstructions in Sect. 4.

## 2 Isotope data and modeling

### 2.1 Ice core isotopic data

We used the three deep ice cores drilled in East Antarctica, DF, Vostok and EDC. The DF data were extended and revised in this paper. Two ice cores were drilled at the DF station ( $77^\circ 19' \text{S}$ ,  $39^\circ 42' \text{S}$ , elevation 3810 m). The first 2503 m-depth core (DF1) was drilled in 1996, and revealed the  $\delta^{18}O$  and  $\delta D$  records back to  $\sim 340$  kyr

394

BP (thousands of years before present) (Watanabe et al., 2003; Uemura et al., 2004). Then, the other core (Dome Fuji 2nd, DF2) reached near bedrock in 2007 at the depth of 3035.2 m (Motoyama, 2007), and its  $\delta^{18}\text{O}$  record from a  $\sim 130$  m-length (2399.5–2531.5 m depth) core was published (Uemura et al., 2010). Here, we show  $\delta\text{D}$  and  $d$  records from this  $\sim 130$  m-length part of the DF2 core at 10 cm-length sampling from every 50 cm ( $n = 265$ ). The  $\delta\text{D}$  data from the overlapping part (2400–2500 m) shows remarkable similarity between DF1 and DF2 (Fig. 1).

The DF isotope ratios were measured using an equilibration method (Uemura et al., 2007) at National Institute of Polar Research, Japan. Routine measurements (2006 to 2008) of a reference water sample show that reproducibilities ( $1\sigma$ ) of this water are 0.3‰ for  $\delta\text{D}$ , 0.04‰ for  $\delta^{18}\text{O}$ , and 0.4‰ for  $d$ . Duplicate analyses for 119 ice core samples confirm these estimates. In order to obtain the revised  $d$  record for the entire DF core, a new data set was made by 1) subtracting artificial isotope offsets from DF1 record (see below) and 2) replacing the DF1 data by DF2 data for overlapping part (2400–2503 m). First, there are offsets between DF1 and DF2 ( $\delta_{\text{DF1}} - \delta_{\text{DF2}} = 0.8\text{‰}$  for  $\delta\text{D}$ , and 0.24‰ for  $\delta^{18}\text{O}$ ). Re-measurement of DF1  $\delta$  values, based on  $\sim 60$  samples re-cut from the archived DF1 core, were consistent with that of DF2 data, but larger than that of old DF1 data. Therefore, the gap could be caused by problems in the storage of the DF1 samples preserved in glass vials as liquid. The offsets of  $\delta$  values were subtracted from the published data (Watanabe et al., 2003; Uemura et al., 2004). Second, an enlarged view of the records clearly shows that the  $d$  data are less noisy for DF2 than for DF1, suggesting that the precision of the new data is improved by replicate measurements of many ( $\sim 30\%$ ) samples (Fig. 1). Thus, we replaced DF1 record by DF2 for the overlapping period.

For Vostok (78°30' S, 106°54' E, elevation 3488 m), the  $d$  data are available back to  $\sim 420$  kyr BP (Vimeux et al., 2001). We restricted the ice core comparison over the past 250 kyr because the deeper part of the data is likely affected by changes in ice origin due to ice flow (Vimeux et al., 2001). For the EDC core (75°06' S, 123°23' E, elevation 3233 m), we used the recently published record spanning over 140 kyr BP (Stenni et al.,

395

2010). Another  $d$  record from EDML (75°00' S, 00°09' E, elevation 2892 m) is also available for the same period but was not considered here because of uncertainties in elevation/ice origin impact (Stenni et al., 2010).

Precision of  $\delta^{18}\text{O}$  and  $\delta\text{D}$  measurements of both the Vostok and EDC cores are 0.05‰ and 0.5‰ respectively (Vimeux et al., 2001; Stenni et al., 2010) with a final precision of 0.6‰ on  $d$ . Therefore, the isotopic precisions of the three ice cores are similar. The temporal-resolution of the data sets, however, differs one from the other. The average temporal-resolution of the DF data is  $\sim 270$  yr, except for the  $\sim 70$  yr resolution during the Holocene. For Vostok, the average temporal resolution is smaller than  $\sim 220$  yr for our period of interest (Vimeux et al., 2001). The EDC core shows the highest temporal resolution;  $\sim 18$  yr for the Holocene,  $\sim 50$  yr for MIS2 and  $\sim 42$  yr for MIS5.5 (Stenni et al., 2010).

The comparison of the ice core isotopic records first requires to place them on a common age scale. As shown in Fig. 2, significant differences (up to  $\sim 5$  kyr) exist between the glaciological age scales established for Vostok (GT4 age-scale by Petit et al., 1999) and for EDC (EDC3 age-scale by Parrenin et al., 2007) and the  $\text{O}_2/\text{N}_2$  orbital age scale for DF (Kawamura et al., 2007). Here, we use the DF age scale as a target and synchronized the Vostok, EDC and our new stacked DF record using visual  $\delta\text{D}$  matching (Fig. 2). We used 21 tie points for DF-Vostok fitting. The difference of the age-scales is  $\sim 1$  kyr before 80 kyr BP, and increased up to  $\sim 5$  kyr around 120 kyr BP. We used nine tie points for DF-EDC fitting. The difference of the age-scales is  $\sim 1$  kyr before 80 kyr BP, and increased up to  $\sim 4$  kyr for the older part. For the calculation of  $\Delta T_{\text{site}}$  and  $\Delta T_{\text{source}}$ , all the data were re-sampled with 200-yr resolution, which is under-sampling for EDC data, and slightly over-sampling for Vostok and DF data.

## 2.2 Raw $d$ -excess and $\delta\text{D}$ data

The raw  $d$  records from the DF, Vostok, and EDC ice cores show common low frequency variability ( $\sim 40$  kyr) (Fig. 2). This obliquity imprint is significantly smaller in DF than in the Vostok and EDC cores. In particular, minima of DF  $d$  record at about 20, 40,

396

and 90 kyr BP are less distinct. Such difference, however, cannot be found in the older section (200–250 kyr BP) of DF and Vostok. Another difference can be found during the glacial terminations. From 20 to 10 kyr BP (Termination I), the onset of  $d$  increases in DF and Vostok appears to lag that of EDC. From 140 kyr to 130 kyr BP (Termination II), a similar lag is observed. It is difficult to interpret the raw  $d$  record because it is an empirically defined second-order parameter. In fact, a different definition of  $d$  parameter can produce different glacial interglacial variations (see Sect. 3 and Appendix A). Climatic interpretation of  $d$  will be discussed after inferring  $\Delta T_{\text{source}}$  from isotopic data (Sect. 4).

### 2.3 Isotope inversion method

In order to retrieve the climatic information from the isotope ratios, we need to evaluate several coefficients using an isotope model. Sensitivities of  $\delta D$  and  $d$  to  $\Delta T_{\text{site}}$ ,  $\Delta T_{\text{source}}$ , relative humidity (RH), and ocean isotopic composition ( $\delta^{18}\text{O}_{\text{sw}}$ ) were estimated using a mixed cloud isotopic model (MCIM) developed by Ciais and Jouzel (1994). We used a linear inversion method which is very similar procedure performed for Vostok (Cuffey and Vimeux, 2001) and EDC records (Stenni et al., 2001, 2003, 2010; Masson-Delmotte et al., 2004).

There are several differences among the inversion methods used for various ice cores. First, the coefficients for the correction for  $\delta^{18}\text{O}_{\text{sw}}$  were used as fixed parameters in several studies (Vimeux et al., 2001, 2002; Cuffey and Vimeux, 2001; Stenni et al., 2001). This coefficient, however, can be exactly calculated as a function of the isotopic composition of the ice (Vimeux et al., 2001; Jouzel et al., 2003; Kavanaugh and Cuffey, 2003), as follows:

$$\delta^{18}\text{O}_{\text{corr}} = \delta^{18}\text{O}_{\text{ice}} - \delta^{18}\text{O}_{\text{sw}} \frac{(1 + \delta^{18}\text{O}_{\text{ice}})}{(1 + \delta^{18}\text{O}_{\text{sw}})} \quad (1)$$

397

$$\delta D_{\text{corr}} = \delta D_{\text{ice}} - \delta D_{\text{sw}} \frac{(1 + \delta D_{\text{ice}})}{(1 + \delta D_{\text{sw}})} \quad (2)$$

Here,  $\delta^{18}\text{O}_{\text{corr}}$  and  $\delta D_{\text{corr}}$  are the isotope ratios of the ice ( $\delta^{18}\text{O}_{\text{ice}}$  and  $\delta D_{\text{ice}}$ ) corrected for ocean isotope changes ( $\delta^{18}\text{O}_{\text{sw}}$  and  $\delta D_{\text{sw}}$ ). An estimate of the global ice volume component of sea-water  $\delta^{18}\text{O}$  (Bintanja and Wal, 2008) was used for the  $\delta^{18}\text{O}_{\text{sw}}$  record. The  $\delta D_{\text{sw}}$  can be calculated on the assumption that  $\delta D_{\text{sw}} = 8 \times \delta^{18}\text{O}_{\text{sw}}$ . Thus, the  $d$  value corrected for the ocean isotope effect ( $d_{\text{corr}}$ ) can be obtained by:  $d_{\text{corr}} = \delta D_{\text{corr}} - 8\delta^{18}\text{O}_{\text{corr}}$ . Following recent studies (e.g. Stenni et al., 2010), we apply this correction before conducting the multiple linear regression.

Second,  $\delta D$  and  $d$  in polar precipitation preserve source effects and therefore depends on climatic parameters affecting evaporation kinetics, including  $\Delta T_{\text{source}}$  but also relative humidity (RH) and wind-speed regimes (Merlivat and Jouzel, 1979; Petit et al., 1991). For Vostok, the RH effect was explicitly included in the  $\Delta T_{\text{source}}$  by using a linear relation found in outputs of Atmospheric General Circulation Models ( $\Delta h \sim -0.4\Delta T_{\text{source}}$ ) (Vimeux et al., 2001; Cuffey and Vimeux, 2001). For EDC, the RH effect was not included, restricting the analyses of source effects to  $\Delta T_{\text{source}}$  only (Stenni et al., 2001). Here, we adopted the latter approach for the sake of simplicity. Thus, the results of multiple linear regressions can be expressed as:

$$\Delta \delta D_{\text{corr}} = \gamma_{\text{site}} \Delta T_{\text{site}} - \gamma_{\text{source}} \Delta T_{\text{source}} \quad (3)$$

$$\delta d_{\text{corr}} = -\beta_{\text{site}} \Delta T_{\text{site}} + \beta_{\text{source}} \Delta T_{\text{source}} \quad (4)$$

All the  $\gamma$  and  $\beta$  coefficients are positive numbers expressed in  $\text{‰} \text{K}^{-1}$ . The  $\Delta$  represents deviations from the present reference values (in this study “present” is defined as the averaged value of the past 2 kyr). The  $\Delta T_{\text{site}}$ , mean annual temperature at ground level, is calculated from the mean annual temperature of condensation ( $\Delta T_{\text{c}}$ ) by assuming a constant relation ( $\Delta T_{\text{c}} = 0.67\Delta T_{\text{site}}$ ) (Jouzel and Merlivat, 1984). This is of course an approximation as Antarctic inversion strength varies through places, time and weather conditions. A detailed analysis of condensation temperature conducted

398

using half-century-long meteorological observations from Vostok (Ekaykin, 2003) recently confirmed the validity of this approach for this site.

Finally, a kinetic isotope fractionation occurs during ice crystal growth because of super-saturation over ice, parameterized as a linear function of temperature and tuned to reproduce the spatial  $d$  vs.  $\delta$  distribution in Antarctica (Petit et al., 1991). We used a linear function ( $S_i = 1.020 - 0.0037T$ ) which best reproduces the present-day surface snow  $d$  vs.  $\delta D$  distribution from various parts of Antarctica (Masson-Delmotte et al., 2008), and from the Japanese-Swedish IPY 2007/2008 traverse (Fujita et al., 2011) covering the Syowa-Dome F route (Fig. 3). In this study, all the simulations were conducted using this fixed super super-saturation function.

## 2.4 Present-day isotope tuning

The first step for estimating the sensitivity coefficients is to fit the model output to the present-day snow isotopic distribution (Fig. 3). An important problem of this tuning is the difficulty to simulate present-day snow isotope ratios by using the MCIM. At the DF site, the present-day (past 2 kyr average  $\pm 1\sigma$ ) isotope ratios are  $\delta^{18}\text{O} = -55.09 \pm 0.16\text{‰}$ ,  $\delta D = -426.3 \pm 1.4\text{‰}$ , and  $d = 14.4 \pm 0.3\text{‰}$ . With our MCIM tuning, these isotope ratios can only be reached with a very cold site temperature,  $-61.0^\circ\text{C}$ , which is significantly lower than the 10 m-depth temperature of  $-57.7^\circ\text{C}$  (Motoyama et al., 2005) and 1-yr observations at 4 m-height of  $-54.8^\circ\text{C}$  (Fujita and Abe, 2006). The difficulties to simulate present-day  $\delta$  values might also reflect the difference between annual mean temperature and precipitation weighted temperature (e.g. Masson-Delmotte et al., 2011), and/or differences in prescribed surface air-pressures. In fact, the air pressure of DF is the lowest among the coring sites since its elevation is the highest (3810 m a.s.l.) compared with the VK (3488 m a.s.l.) and EDC (3233 m a.s.l.). Lower air-pressure results in smaller distillation in the model, and thus produces higher simulated  $\delta$  values.

399

We have therefore two options. Either we use a “realistic” DF temperature and perform regressions in an isotope range that is not sufficiently depleted when compared to the data; or we use colder than observed temperatures (and associated fractionation coefficients) to perform the regressions on the isotopic model results. Here, we explore the impacts of the second option of an “isotope fitted” procedure. We note that, as calibration targets, averaged isotope ratios are more reliable compared to Antarctic annual-mean temperature data due to the short instrumental records for instance at DF. In the temperature range encountered in Central East Antarctica, fractionation coefficients are extrapolated from values measured in laboratory experiments (with the coldest temperature of  $-40^\circ\text{C}$  and  $-33.4^\circ\text{C}$  for deuterium, Merlivat and Nief, 1967; and oxygen-18, Majoube, 1971b; respectively). These fractionation coefficients are thus not precisely known for very low temperatures and associated uncertainties should be kept in mind.

## 3 Uncertainty on the sensitivity of $d$ to temperature

### 3.1 Sensitivity of $\beta_{\text{site}}$ estimation

In the multiple linear regressions (Eqs. 3 and 4), a major source of uncertainty lies in the coefficient of regression,  $\beta_{\text{site}} (= \partial d / \partial \Delta T_{\text{site}})$  which is related to the sensitivity of  $d$  to  $\Delta T_{\text{site}}$ . Table 1 shows that  $\beta_{\text{site}}$  values published in previous studies are significantly different, ranging from  $\sim 0.5$  (Cuffey and Vimeux, 2001; Stenni et al., 2001) to 1.2 (Salamatin et al., 2004). Note that some recent studies used new  $^{17}\text{O}$ -excess data to tune the MCIM and obtained larger  $\beta_{\text{site}}$  values (Landais et al., 2009; Risi et al., 2010; Winkler et al., 2012). In principle,  $\beta_{\text{site}}$  depends on the isotopic depletion as the temperature is almost linearly related to  $\delta D$ . Figure 3 shows the  $d$ - $\delta D$  slope increases with isotopic depletion and colder temperature ranges.

To test the  $\beta_{\text{site}}$  sensitivity to temperature changes, the source and site temperatures at DF were changed without changing any tuning parameters (Table 2). We tuned the

400





remove several (1 to 5) points located around the “corner” of data subset (Fig. 4), the uncertainties of the linear coefficients are 0.01 to 0.04. Such statistical regression error analysis, however, does not represent the total uncertainties on the estimated  $\Delta T_{\text{site}}$  and  $\Delta T_{\text{source}}$ . It does not account for uncertainties on MCIM parameterization tunings (e.g. supersaturation), and on climate parameters not taken into account (precipitation intermittency, inversion strength, changes in wind speed and/or relative humidity. For example, Winkler et al. (2011) show that the  $\beta_{\text{site}}$  depends on the tuning of supersaturation, and an error range was estimated as 1.29 to 2.04.

We have also applied the exact same methodology for EDC and Vostok, using the same tuning of MCIM and performing the linear analyses on the range of model outputs consistent with each ice core isotopic dataset. Table 1 compares our results with previous regressions. Among four coefficients in the equations, only  $\beta_{\text{site}}$  is significantly different from previous estimate, which is now 2.5 times larger than previous one ( $\sim 0.5$ ). As discussed in Sects. 3.1 and 3.2, differences found in  $\beta_{\text{site}}$  between previous studies can be explained by the different methodologies: whether the model is tuned to reproduce the isotope ratios or air-temperature.

The value of  $\beta_{\text{site}}$ , which seems high for East Antarctica sites, is actually very dependent on the  $d$  definitions and on the range of temperatures studied. To understand the influence of the historical linear definition of  $d$  on the  $\beta_{\text{site}}$ , we tested a logarithmic definition of  $d$  (see Appendix A for detail). The results confirm that the value of  $\beta_{\text{site}}$  significantly depends on the definition of  $d$ . A logarithmic  $d$  definition can remove the influence of  $\Delta T_{\text{site}}$  on  $d$  spatial variations, and thus significantly reduce the value of  $\beta_{\text{site}}$ . But this new definition does not change anything to the temperature reconstructions, because  $\beta_{\text{site}}$  act as a correction factor for the empirically defined  $d$  parameter.

## 4 Reconstructed $\Delta T$ source and $\Delta T$ site

### 4.1 $\Delta T_{\text{source}}$ and $\Delta T_{\text{site}}$ of Dome F

The new coefficients obtained in this study (Eqs. 5 and 6) were applied to the DF ice core data to estimate past variations in  $\Delta T_{\text{source}}$  and  $\Delta T_{\text{site}}$  (Fig. 5). The new  $\Delta T_{\text{source}}$  vary between  $-5.9^{\circ}\text{C}$  to  $2.9^{\circ}\text{C}$  over the past 360 kyr. The record shows maxima of  $\Delta T_{\text{source}}$  occurring during Marine Isotope Stage (MIS) 5e and MIS 9e with values respectively  $2.6 \pm 0.3^{\circ}\text{C}$  and  $2.9 \pm 0.3^{\circ}\text{C}$  higher than present. A glacial minimum at 19 kyr BP is  $-5.9 \pm 0.3^{\circ}\text{C}$ . Here, temperatures are based on the average and  $\pm 1\sigma$  of 1 kyr duration around the maximum or minimum point. This  $\Delta T_{\text{source}}$  reconstruction remains high when  $\Delta T_{\text{site}}$  and  $\delta D$  drop during glacial inceptions, linked with high  $d$  values during the onset of glaciations. The DF  $\Delta T_{\text{site}}$  derived from the new coefficients ranges between  $-7.8 \pm 0.2^{\circ}\text{C}$  to  $4.8 \pm 0.5^{\circ}\text{C}$  over the past 360 kyr. Maximum  $\Delta T_{\text{site}}$  occur during MIS 9e, with temperature  $4.8 \pm 0.5^{\circ}\text{C}$  warmer than that of present-day average.

In order to show the importance of the value of  $\beta_{\text{site}}$ , other  $\Delta T_{\text{source}}$  and  $\Delta T_{\text{site}}$  records which were obtained using the smaller values of  $\beta_{\text{site}}$  (0.5) and other coefficients used in Cuffey and Vimeux (2001) (Table 1) are shown in Fig. 5a. For clarity, we labeled this  $\Delta T_{\text{source}}$  and  $\Delta T_{\text{site}}$  records based on the smaller  $\beta_{\text{site}}$  coefficient as  $\Delta T_{\text{source}}^{\text{low}}$  and  $\Delta T_{\text{site}}^{\text{low}}$ , respectively. Two major differences are identified for the source temperature records. First, the glacial-interglacial amplitude of the new  $\Delta T_{\text{source}}$  is approximately twice larger than that of  $\Delta T_{\text{source}}^{\text{low}}$ . Second, the timing of the interglacial-glacial inception maxima is strongly affected: small  $\beta_{\text{site}}$  coefficients induce a maximum  $\Delta T_{\text{source}}^{\text{low}}$  at the onset of glaciations (MIS 5d), while large  $\beta_{\text{site}}$  coefficients place  $\Delta T_{\text{source}}$  maxima in phase with Antarctic warmth (MIS 5e). With the exception of glacial inceptions, the new  $\Delta T_{\text{source}}$  reconstruction is also much more similar to  $\Delta T_{\text{site}}$ .

In contrast to the sensitivity of  $\Delta T_{\text{source}}$  to the uncertainties in regression coefficients, the  $\Delta T_{\text{site}}$  shows much less sensitivity (Fig. 5c). Indeed, the difference between  $\Delta T_{\text{site}}$  and  $\Delta T_{\text{site}}^{\text{low}}$  is  $\sim 0.6^{\circ}\text{C}$ , which is within typical error ( $-10$ – $30\%$ ) of temperature







our high  $\beta_{\text{site}}$  case, the site-source temperature gradient mainly exhibits obliquity periodicities, which is a requested characteristic for orbital tuning. Cross spectrum analysis shows that the mean lag of this reconstructed gradient behind the obliquity is 2.9 kyr. The gradients of EDC and VK also lag the obliquity by 2.9 and 3.0 kyr, respectively. This differs from the observed 5 kyr lag between EDC  $\delta\text{D}$  and obliquity (Jouzel et al., 2007). The processes responsible for the observed lags remain elusive, and likely involved the interplay between ice sheets and ocean circulation. Further investigations of the mechanisms linking obliquity and site-source temperature gradient should be conducted, in order to use such information for orbital dating of ice cores. It will be important independent evidence to test the length of MIS 11, in which the accuracy of the EDC3 age scale (Parrenin et al., 2007) was questioned (Masson-Delmotte et al., 2010b; Pol et al., 2011).

## 5 Conclusions and perspective

We obtained a new  $d$  record from DF ice core spanning the past 360 000 yr and compared with records from Vostok and EDC ice cores. To interpret the  $d$  and  $\delta\text{D}$  records as  $\Delta T_{\text{source}}$  and  $\Delta T_{\text{site}}$  information, we used an isotopic inversion based on the MCIM model as previously performed by Vimeux et al. (2002); Stenni et al. (2001) on the Vostok and EDC ice cores, respectively. A major source of uncertainty lies in the coefficient of regression,  $\beta_{\text{site}}$  which is related to the sensitivity of  $d$  to  $\Delta T_{\text{site}}$ . We showed that different ranges of temperature and selections of isotopic model outputs may increase the value of  $\beta_{\text{site}}$  by a factor of two. The results suggest that the causes for the differences of  $\beta_{\text{site}}$  between the previous studies lie in the isotopic model tuning for the present-day, and the  $\delta\text{D}$  ranges selected for regression analyses because the  $\beta_{\text{site}}$  depends on the range of temperature or isotopic depletion considered.

For the first time, we applied the exact same temperature inversion methodology to the three Antarctica ice cores data set (DF, Vostok, and EDC). All  $\Delta T_{\text{source}}$  records were very sensitive to the inversion method, with our new approach (isotope-fitting) leading

409

to amplitudes of  $\Delta T_{\text{source}}$  variation  $\sim 2^\circ\text{C}$  to  $4^\circ\text{C}$  larger compared to the previous estimations. For DF, the  $\Delta T_{\text{source}}$  estimates yield values between  $-5.9^\circ\text{C}$  to  $2.9^\circ\text{C}$  over the past 360 kyr. Comparisons with proxy-based SST records suggest that our large  $\Delta T_{\text{source}}$  reconstruction is at the upper limit of compatibility with SST data. In contrast to the significant modification in  $\Delta T_{\text{source}}$ , the  $\Delta T_{\text{site}}$  records were not modified significantly and therefore appear robust. The differences between the current and previous studies are within published uncertainty ( $-10$ – $30\%$ ) of  $\Delta T_{\text{site}}$  estimations. The new  $\Delta T_{\text{source}}$  estimates showed only weak 41-kyr obliquity periodicity, but the obliquity signal was found in the temperature gradient ( $\Delta T_{\text{source}} - \Delta T_{\text{site}}$ ). The temperature gradient records of the three cores show a systematic anti-correlation with obliquity, providing new evidence for the importance of the Earth's obliquity as a driver of water cycle and climate dynamics. Such properties offer the perspective of using this obliquity imprint as a synchronization tool for dating ice cores.

The isotope inversion method involves simplification, and the procedure is challenging, in particular in Antarctica where isotope ratios are extremely depleted. Analyzing  $d$  at an event basis in modern condensing vapor and precipitation could be very useful, combined with moisture tracking analysis (Sodemann and Stohl, 2009) and isotopic modeling, to identify what are the correct or incorrect hypotheses and parameterizations in distillation models regarding the controls of  $d$ . Triple isotope ratios of oxygen (i.e.  $^{17}\text{O}$ -excess) in water molecules (Landais et al., 2008; Luz and Barkan, 2010; Winkler et al., 2012) would also provide independent evidence for moisture source imprint on isotopically depleted snow. Finally, extensive field observation of  $d$  and  $^{17}\text{O}$ -excess in clouds over Antarctica may provide better constraints on supersaturation function, and will allow to improve our understanding of the mechanism underlying the changes in  $d$  and  $^{17}\text{O}$ -excess.

## Appendix A

### Logarithmic definition of $d$ and meaning of $\beta_{\text{site}}$

The interplay of artifacts caused by the empirical  $d$  definition and by physical kinetic processes (evaporation and snow formation) restricts precise physical understanding of meaning to the value of two coefficients ( $\beta_{\text{site}}$  and  $\beta_{\text{source}}$ ) in Eq. (4). The empirical definition (i.e. the constant slope of 8) of  $d$  itself induces changes in  $d$  because any process that does not follow the  $\delta\text{D}/\delta^{18}\text{O}$  slope of 8 alters the  $d$  value. Indeed the  $\delta\text{D}/\delta^{18}\text{O}$  slope can deviate from the mean value of 8 because of the combination of the nonlinearity of the ratio of equilibrium-fractionation factors and the crude approximation of  $\ln(1 + \delta) \sim \delta$ . In contrast to the historical linear definition of  $d$ , recent studies of triple oxygen isotope study of water have used the logarithmic framework for defining the  $^{17}\text{O}$ -excess parameter (Barkan and Luz, 2007). Here, we examine how the historical definition of  $d$  affects the ice core  $d$  record and  $\beta_{\text{site}}$  by introducing a logarithmic based definition of deuterium excess.

In the normal  $\delta$  plot, the slope of Global Meteoric Water Line (GMWL) apparently keeps a constant value “8” along with isotope distillation (Craig, 1961). However, it is difficult to understand the physical meaning of this constant slope because the ratio of equilibrium fractionation-factors of hydrogen and oxygen ( $(\alpha_{\text{D}} - 1)/(\alpha_{18} - 1)$ ), which corresponds to the  $\delta\text{D}/\delta^{18}\text{O}$  slope, increases from 8.7 to 9.6 when the temperature decreases from 20°C to 0°C (e.g. Jouzel, 1986). In principle, the increasing slope should be observed only in the  $\log(1 + \delta)$  plot. This point was clearly described in the historic GMWL paper (Craig, 1961) as; “it is actually  $\log(1 + \delta)$  which should be plotted for such a process ... The linear relation observed in Fig. 1 simply reflects a coincidence”. Recently, the limitation of normal  $\delta$  diagrams is discussed in Miller (2002). In Antarctica,  $-50\text{‰}$  and  $-400\text{‰}$  in  $\delta$  notation (either  $\delta\text{D}$  or  $\delta^{18}\text{O}$ ) corresponds to  $-51.3\text{‰}$  and  $-511\text{‰}$  in  $\log(1 + \delta)$  notation, respectively. Thus,  $\ln(1 + \delta)$  cannot be approximated as  $\delta$ .

411

In order to show the differences of normal and logarithmic plot, global isotope data from Global Network of Isotopes in Precipitation (GNIP) database (e.g. Rozanski et al., 1993) and a recent compilation of Antarctic surface snow data (Masson-Delmotte et al., 2008) are shown in Fig. A1. Although, the GMWL appears to represent average isotopic composition, the slope is, in reality, non-linear. The  $d$  data shows parabolic curve against  $\delta^{18}\text{O}$  with a minimum ( $\sim$  negative values in  $d$ ) at  $\sim -30\text{‰}$  in  $\delta^{18}\text{O}$ , and maxima ( $\sim 15\text{--}20\text{‰}$  in  $d$ ) at  $\sim 0\text{‰}$  (equatorial) and  $\sim -60\text{‰}$  in  $\delta^{18}\text{O}$  (Antarctica) (Fig. A1a). Figure A1b shows the same data but on natural logarithmic plot. The data clearly show non-linear relationship between  $\ln(1 + \delta\text{D})$  vs.  $\ln(1 + \delta^{18}\text{O})$ . A simple quadric fitting gives sufficiently good representation as:

$$\ln(1 + \delta\text{D}) = -2.85 \times 10^{-2} \times (\ln(1 + \delta^{18}\text{O}))^2 + 8.47 \times \ln(1 + \delta^{18}\text{O}) + 13.3 (R^2=0.999). \quad (\text{A1})$$

Unlike a constant slope of GMWL, the slope of this Global Meteoric Water Curve (GMWC) increases from  $\sim 8.5$  to 12 as  $\ln(1 + \delta^{18}\text{O})$  decreases. Figure A2 shows the slope and  $\ln(1 + \delta^{18}\text{O})$  with corresponding annual-mean surface air-temperature. This slope generally agrees with the one expected from  $(\alpha_{\text{D}} - 1)/(\alpha_{18} - 1)$ . There is a clear gap between the transition of equilibrium fractionation factors for liquid-vapor and ice-vapor for  $^{18}\text{O}$  (Majoube, 1971a, b) and for D (Merlivat and Nief, 1967). The gap was narrowed after incorporating the super saturation effect (Jouzel and Merlivat, 1984) (here, we used the  $S_i$  function described in Sect. 2.2 was used).

Based on the GMWC, a deuterium-excess paramter based on logarithmic  $\delta$ , hereafter denoted as  $d_{\text{ln}}$ , is defined as:

$$d_{\text{ln}} = \ln(1 + \delta\text{D}) - (-2.85 \times 10^{-2} \times (\ln(1 + \delta^{18}\text{O}))^2 + 8.47 \times \ln(1 + \delta^{18}\text{O})). \quad (\text{A2})$$

In contrast to the  $d$ , which shows parabolic curve against  $\delta^{18}\text{O}$ ,  $d_{\text{ln}}$  does not depend on  $\ln(1 + \delta^{18}\text{O})$  (Fig. A1b). Note that  $d_{\text{ln}}$  is defined based on phenomenological data set. Thus, not only the equilibrium effect but also kinetic fractionation (like snow formation effect) is also eliminated.

Figure A3 shows the  $d_{\text{ln}}$  records of Antarctic ice cores. The  $d_{\text{ln}}$  ranges from about  $-15\text{‰}$  to  $5\text{‰}$ . The glacial-interglacial amplitude is, thus, about two times larger than

412











- from the Dome Fuji ice core, Antarctica, *Geochim. Cosmochim. Acta*, 74, 4919–4936, doi:10.1016/j.gca.2010.05.007, 2010.
- Vázquez Riveiros, N., Waelbroeck, C., Skinner, L., Roche, D. M., Duplessy, J.-C., and Michel, E.: Response of South Atlantic deep waters to deglacial warming during Terminations V and I, *Earth Planet. Sci. Lett.*, 298, 323–333, doi:10.1016/j.epsl.2010.08.003, 2010.
- Vimeux, F., Masson, V., Jouzel, J., Stievenard, M., and Petit, J. R.: Glacial-interglacial changes in ocean surface conditions in the Southern Hemisphere, *Nature*, 398, 410–413, 1999.
- Vimeux, F., Masson, V., Delaygue, G., Jouzel, J., Petit, J. R., and Stievenard, M.: A 420 000 year deuterium excess record from East Antarctica: information on past changes in the origin of precipitation at Vostok, *J. Geophys. Res.*, 106, 31863–31873, 2001.
- Vimeux, F., Cuffey, K. M., and Jouzel, J.: New insights into Southern Hemisphere temperature changes from Vostok ice cores using deuterium excess correction, *Earth Planet. Sci. Lett.*, 203, 829–843, 2002.
- Watanabe, O., Jouzel, J., Johnsen, S., Parrenin, F., Shoji, H., and Yoshida, N.: Homogeneous climate variability across East Antarctica over the past three glacial cycles, *Nature*, 509–512, 2003.
- Winkler, R., Landais, A., Sodemann, H., Dümbgen, L., Prié, F., Masson-Delmotte, V., Stenni, B., and Jouzel, J.: Deglaciation records of  $^{17}\text{O}$ -excess in East Antarctica: reliable reconstruction of oceanic normalized relative humidity from coastal sites, *Clim. Past*, 8, 1–16, doi:10.5194/cp-8-1-2012, 2012.

421

**Table 1.** Comparison of the temperature inversion coefficients.

Site	$\beta_{\text{site}}$	$\beta_{\text{source}}$	$\beta_{\text{sw}}$	$Y_{\text{site}}$	$Y_{\text{source}}$	$Y_{\text{sw}}$	Reference
DF	1.3	1.6		7.7	3.2	–	This study
Vostok <sup>1</sup>	0.5	1.3	2.8	7.1	3.7	4.8	Cuffey and Vimeux (2001); Vimeux et al. (2002)
Vostok <sup>1,2</sup>	0.9, 1.2	1.1, 1.2	3.0, 2.9	6.8, 6.9	2.8, 3.6	4.5, 4.7	Salamantin (2004)
Vostok <sup>1,3</sup>	1.0	1.4	3	–	–	–	Landais et al. (2009)
Vostok <sup>3</sup>	1.1	1.5	–	–	–	–	Risi et al. (2010)
Vostok	1.4	1.6	–	7.7	3.1	–	This study
EDC <sup>1</sup>	0.5	1.3	2.6	7.6	3.5	5.0	Senni et al. (2001); Masson (2004)
EDC	0.5	1.3	–	7.6	3.6	–	Stenni et al. (2003)
EDC	1.2	1.5	–	7.8	3.4	–	This study
East Antarctica <sup>1,3</sup>	1.29–2.04	1.31–1.5	3	–	–	–	Winkler et al. (2011)

<sup>1</sup> Corrections for ocean isotope changes were estimated using  $\beta_{\text{sw}}$  and  $Y_{\text{sw}}$ :  $\delta d = -\beta_{\text{site}}\Delta T_{\text{site}} + \beta_{\text{source}}\Delta T_{\text{source}} - \beta_{\text{sw}}\Delta\delta^{18}\text{O}_{\text{sw}}$ , and  $\Delta\delta D = Y_{\text{site}}\Delta T_{\text{site}} - Y_{\text{source}}\Delta T_{\text{source}} + Y_{\text{sw}}\Delta\delta^{18}\text{O}_{\text{sw}}$ . See Sect. 2.3 for detail.

<sup>2</sup> Condensation temperature at precipitation deposition site ( $\Delta T_{\text{c}}$ ) used in original paper was converted to temperature at ground level ( $\Delta T_{\text{site}}$ ) using a linear relation  $\Delta T_{\text{c}} = 0.67\Delta T_{\text{site}}$  (Jouzel and Merlivat, 1984). Thus, the  $d/T_{\text{c}}$  slopes (1.7 and 1.4 for 2 different trajectories) correspond to the values of 1.2 and 0.9 for  $\beta_{\text{site}}$ .

<sup>3</sup> Variations of relative humidity was estimated as an independent parameter.

422

**Table 2.** Test of  $\beta_{\text{site}}$  sensitivity to the source and site temperatures.

Tuning strategy	Simulated DF isotope ratio			Temperatures (°C)		Sensitivity coefficient			
	$\delta D(\text{‰})$	$\delta^{18}\text{O}(\text{‰})$	$d(\text{‰})$	DF site	Source	$\beta_{\text{site}}$	$\beta_{\text{source}}$	$\gamma_{\text{site}}$	$\gamma_{\text{source}}$
Isotope fitted	-422.7	-54.6	14.5	-61	18	1.3	1.6	7.7	3.2
Temperature fitted 1	-377.1	-46.2	6.5	-55	18	0.8	1.3	7.6	3.4
Temperature fitted 2	-351.1	-43.9	-0.2	-55	11	0.6	1.2	7.9	4.1

423

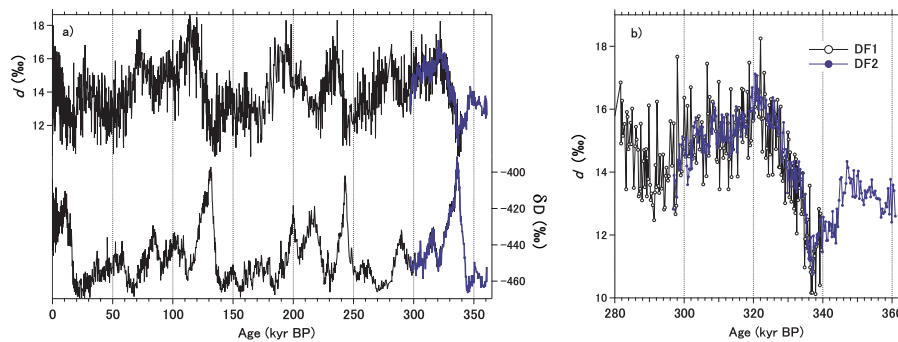


**Fig. 1.**  $\delta D$  and deuterium-excess records from the DF ice cores. **(a)**  $\delta D$  and  $d$  records from DF1 (black lines) and DF2 (blue lines) cores. **(b)** Enlarged view of the  $d$  records during the overlapping period. Here,  $\delta = R_{\text{sample}}/R_{\text{VSMOW}} - 1$ , and  $R_{\text{sample}}$  and  $R_{\text{VSMOW}}$  are the isotope ratios ( $D/H$  and  $^{18}\text{O}/^{16}\text{O}$ ) of sample and VSMOW, respectively.

424

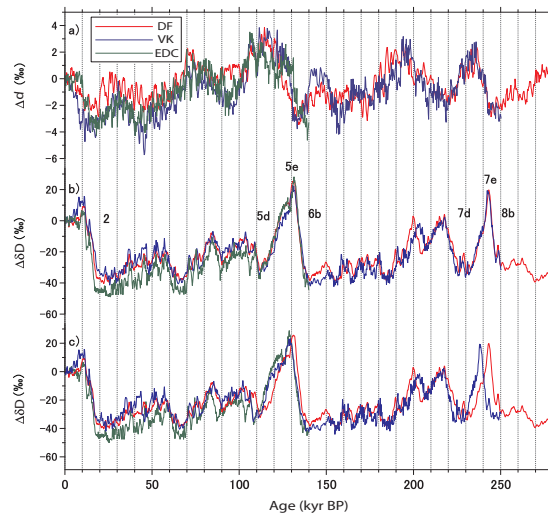


**Fig. 2.** Deuterium-excess and  $\delta D$  records of Antarctic ice cores. **(a)** Deuterium-excess ( $d$ ) records from DF (red line), Vostok (blue line), and EDC (green line) cores plotted on the  $O_2/N_2$  orbital age scale for DF. **(b)**  $\delta D$  records of the three cores plotted on the  $O_2/N_2$  orbital age scale for DF. **(c)**  $\delta D$  records of the three cores plotted on the original age-scales (see text). Numbers indicates corresponding Marine Isotope Stage (MIS) (Tzedakis et al., 2004). All the isotope ratios are expressed as the deviations ( $\Delta$ ) from the present (past 2 kyr average) value.

425

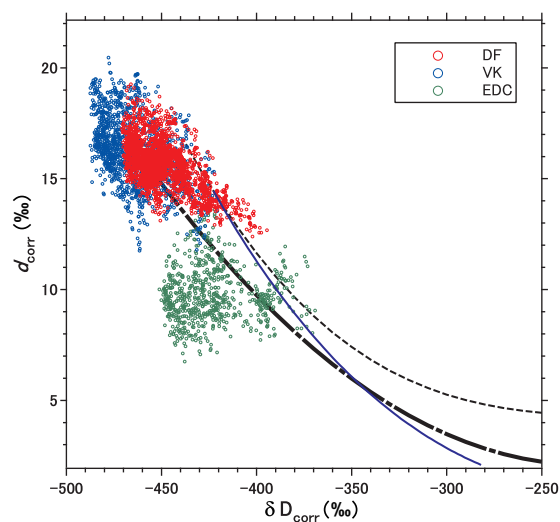


**Fig. 3.** Isotope ratios of Antarctic surface snow and ice cores. Regression curves of surface snow data from various parts of Antarctica (black dashed-dotted line) (Masson-Delmotte et al., 2008), and from Japanese-Swedish IPY 2007/2008 traverse covering Syowa-Dome F route (black dotted line). A simulated curve is shown as blue solid line. Dots represent ice-core data of DF over the past 360 kyr (red), Vostok over the past 250 kyr (blue), and EDC over the past 140 kyr (green). Here,  $\delta D$  and  $d$  are corrected for  $\delta^{18}O_{sw}$ , see text for detail.

426



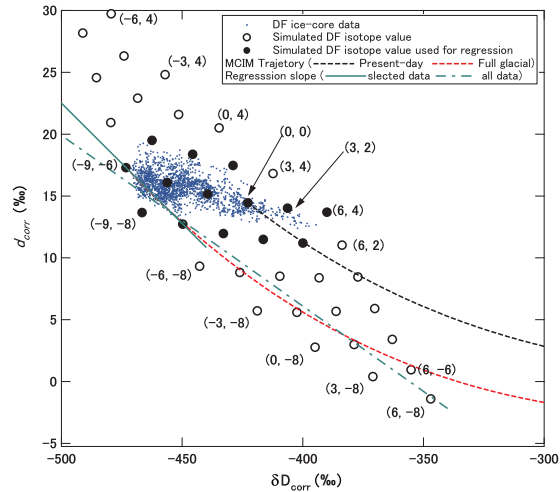


**Fig. 4.** Simulated  $\delta D$  and  $d$  values in Antarctica. Trajectories of present-day (black dotted line) and glacial conditions (red dotted line) are shown. Each point (solid or open circles) represents the simulated snow isotope values at DF site under a specific site and source temperature setting, shown as  $(\Delta T_{\text{site}}, \Delta T_{\text{source}})$  in  $^{\circ}\text{C}$ . The DF ice core data (blue dot), and data used for regression analysis were shown as black solid circle. Linear regression  $d/\delta D$  slopes of a constant  $\Delta T_{\text{source}} (= -6.0^{\circ}\text{C})$  obtained for the filled circles and all circles are shown as green solid and chain lines, respectively. Here,  $\delta D$  and  $d$  are corrected for  $\delta^{18}\text{O}_{\text{SW}}$ , see text for detail.

427

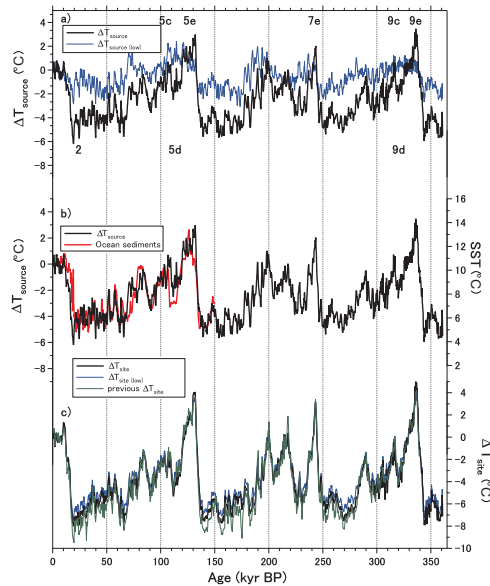


**Fig. 5.** Different  $\Delta T_{\text{source}}$  and  $\Delta T_{\text{site}}$  of DF and a stacked SST records. **(a)** Black line represents the  $\Delta T_{\text{source}}$  record of DF core based on the coefficients ( $\beta_{\text{site}} = 1.3$ ) obtained by isotope-fitting (this study). Blue line represents the  $\Delta T_{\text{source}}^{\text{low}}$  record of DF core based on the coefficients ( $\beta_{\text{site}} = 0.5$ ) used for Vostok reconstruction (temperature-fitting) (Cuffey and Vimeux, 2001; Vimeux et al., 2002). Numbers indicate Marine Isotope Stages. **(b)** Black line is the  $\Delta T_{\text{source}}$  of DF core, same as **(a)**, but with a stacked southern SST record of ocean sediments (Barrows et al., 2007) (red line). **(c)** The  $\Delta T_{\text{site}}$  record based on the coefficients of this study (black line),  $\Delta T_{\text{site}}^{\text{low}}$  (blue line), and previous  $\Delta T_{\text{site}}$  reconstruction of DF core (temperature-fitting) (Kawamura et al., 2007).

428

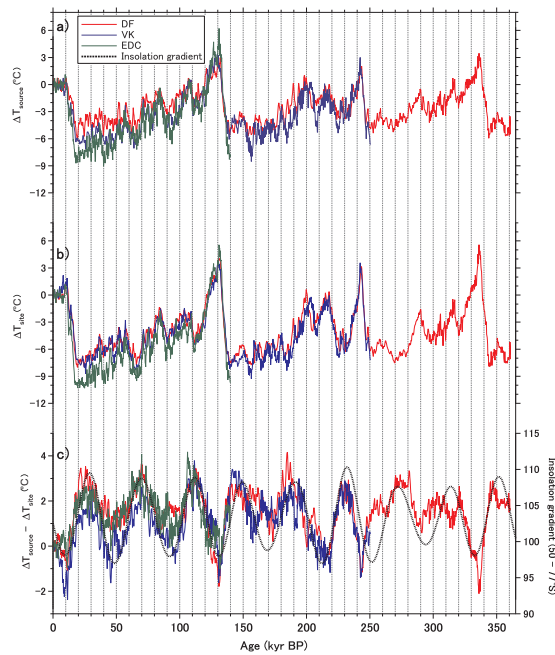


**Fig. 6.** The  $\Delta T_{\text{site}}$ ,  $\Delta T_{\text{source}}$ , and the temperature gradient derived from three cores. Temperature records reconstructed from the DF (red line), Vostok (blue line), and EDC (green line) cores using the isotope-fitting method. **(a)**  $\Delta T_{\text{source}}$ , **(b)**  $\Delta T_{\text{site}}$ , **(c)** Temperature gradient ( $= \Delta T_{\text{source}} - \Delta T_{\text{site}}$ ) and annual mean insolation gradient between 50 and 77° S ( $\text{W m}^{-2}$ , black dotted line).

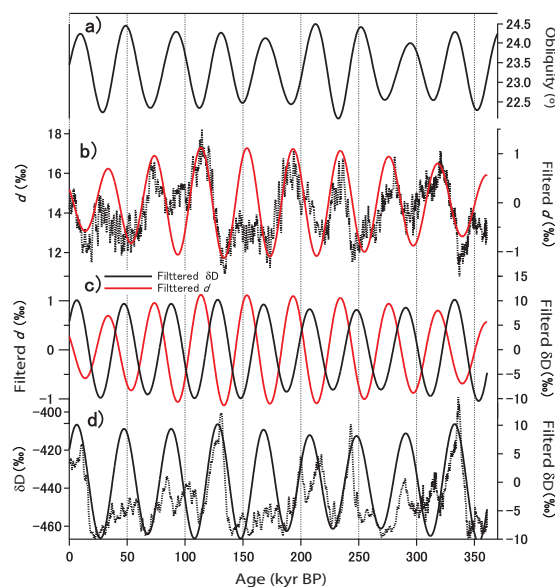


**Fig. 7.** Obliquity components of the DF isotope records. **(a)** Earth's obliquity. **(b)** The raw  $d$  record of DF (black dotted line) and its filtered signal (red solid line). The filtered obliquity component was obtained by Gaussian filters with the AnalyseSeries program (Paillard et al., 1996). A band-pass filter in the obliquity band ( $f = 0.025 \pm 0.005$ ) was calculated (red solid line). **(c)** Filtered components in the DF  $d$  (red solid line) and  $\delta D$  (black solid line). **(d)** The  $\delta D$  (black dotted line) record of DF and its filtered signal (black solid line).

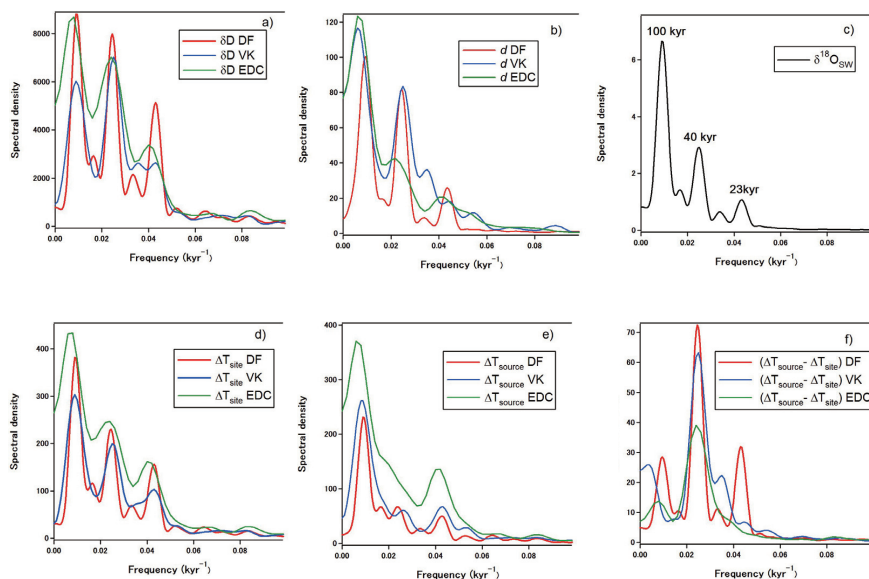


**Fig. 8.** Power spectra of DF core isotope records. Power spectra of DF (red), Vostok (blue), and EDC (green); **(a)**  $\delta D$ , **(b)**  $d$ , **(c)** Ocean isotope change ( $\delta^{18}O_{SW}$ ) over the past 360 kyr (Bintanja and Wal, 2008), **(d)**  $\Delta T_{site}$ , **(e)**  $\Delta T_{source}$ , and **(f)** temperature gradient ( $\Delta T_{source} - \Delta T_{site}$ ). Spectral analysis is performed using Blackman–Tukey analysis with 50 % of series lag (for DF, VK, and  $\delta^{18}O_{SW}$ ) and 70 % (for EDC) with the Anlyseries software (Paillard et al., 1996).

431

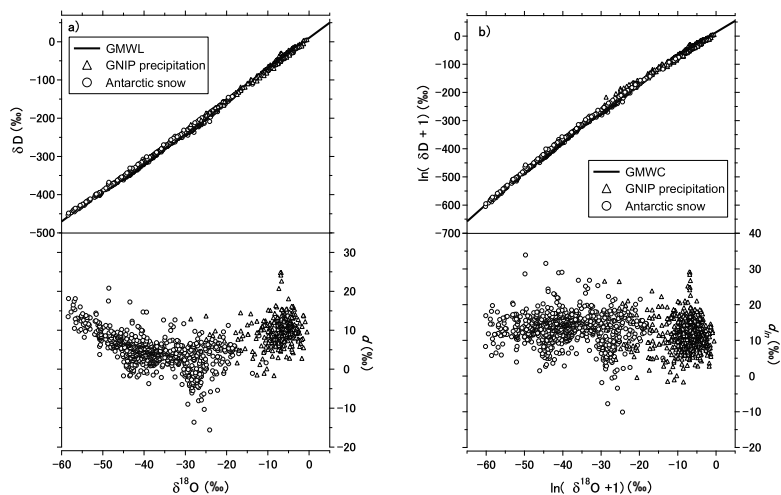


**Figure A1.** Normal versus log plots for global meteoric water. **(a)** GMWL data from GNIP and Antarctic surface snow. GNIP data is based on 308 stations whose data contains the  $d$  data longer than 2 yr. The GNIP data weighted by amount of precipitation give a recession line ( $\delta D = 8.18 \times \delta^{18}O + 11.2 (R^2=0.991)$ ). **(b)** Same as **(a)** but plot on the log plot. All the data give a regression curve (GMWC):  $\delta D = -2.85 \times 10^{-2} \times (\delta^{18}O)^2 + 8.47 \times \delta^{18}O + 13.3 (R^2=0.999)$ .

432

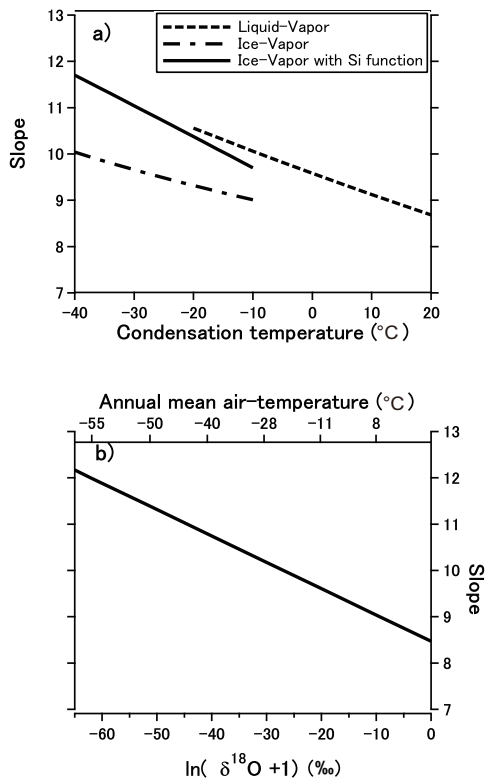


**Figure A2.** Slopes based on fractionation factors and GMWC. The  $\delta D/\delta^{18}O$  slope is calculated using a differential of Eq. (7) ( $= -5.70 \times 10^{-2} \times \ln(1 + \delta^{18}O) + 8.47$ ). Kinetic fractionation during snow formation was considered using a super-saturation function (see text).

433

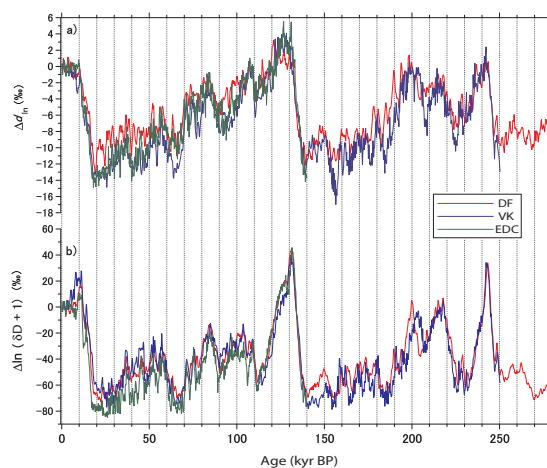


**Figure A3.** Logarithmic defined deuterium-excess and  $\delta D$  records of Antarctic ice cores. **(a)** Deuterium-excess based on logarithmic expression ( $d_n$ ) records from DF (red line), Vostok (blue line), and EDC (green line) cores plotted on the  $O_2/N_2$  orbital age scale for DF. **(b)**  $\ln(\delta D + 1)$  records of the three cores plotted on the  $O_2/N_2$  orbital age scale for DF.

434